### 1

# Femtosecond-laser-induced formation of visible-light-emitting structures inside silicon

Tao Chen, An Pan, Cunxia Li, Jinhai Si\*, and Xun Hou

Abstract—We report 680-nm photoluminescence (PL) from a femtosecond-laser-modified region inside silicon. Light-emitting structures were formed inside silicon by femtosecond laser irradiation in an air atmosphere. The formation of light-emitting structures arose from laser-induced oxygen doping, and doping depths of a few hundred micrometers could be reached. PL intensities increased with increasing depth in the laser-modified region. The effects of the laser powers and scanning velocities were investigated. The peak positions of PL spectra showed almost no change after annealing. According to the Raman spectroscopy analysis, the defect states between the silicon nanocrystals and SiO<sub>2</sub> matrix contribute to the PL.

Index Terms—Photoluminescence, silicon, silicon-rich silica, ultrafast optics, femtosecond laser processing.

### I. INTRODUCTION

Silicon has been one of most important materials in the field of optoelectronics. However, the luminescence efficiency of bulk silicon is very low because of its indirect band gap structure. Numerous Si-based light emitters have been developed by producing low-dimensional silicon systems, such as porous silicon [1], silicon nanoparticles [2, 3] and silicon nanocrystals embedded in a SiO<sub>2</sub> matrix [4–8]. Recently, femtosecond-laser processing has become an attractive method for enhancing the luminescence of silicon. One method of producing light-emitting silicon is to form silicon nanoparticles with a size of a few nanometers by fs-laser ablation of a solid target in a liquid environment [3]. The other method is to form femtosecond-modified structures on a bulk silicon surface [4–6] or silicon compound films [7]. As compared to silicon nanoparticles, the light-emitting

This work was supported by the Collaborative Innovation Center of Suzhou Nano Science and Technology. The authors gratefully acknowledge the financial support for this work provided by the National Basic Research Program of China (973 Program) under Grant No. 2012CB921804 and by the National Natural Science Foundation of China (NSFC) under Grant Nos. 11204236 and 61308006. The authors sincerely thank Ms. Dai at International Center for Dielectric Research (ICDR) in Xi'an Jiaotong University for the support of SEM and EDS measurements.

Tao Chen, An Pan, Jinhai Si\*, and Xun Hou are with Key Laboratory for Physical Electronics and Devices of the Ministry of Education & Shaanxi Key Lab of Information Photonic Technique, School of Electronics & Information Engineering, Xi'an Jiaotong University, No.28, Xianning West Road, Xi'an, 710049, China (email: <a href="mailto:tchen@mail.xjtu.edu.cn">tchen@mail.xjtu.edu.cn</a>; <a href="mailto:pancat@stu.xjtu.edu.cn">pancat@stu.xjtu.edu.cn</a>; <a href="mailto:jinhaisi@mail.xjtu.edu.cn">jinhaisi@mail.xjtu.edu.cn</a>; <a href="mailto:houxun@mail.xjtu.edu.cn">houxun@mail.xjtu.edu.cn</a>).

Cunxia Li is with Departments of Applied Physics, Xi'an University of Technology, Yanxiang Road 58, Xi'an, 710048, China (email: licunxia@xaut.edu.cn).

\*Corresponding author: Jinhai Si (e-mail: jinhaisi@mail.xjtu.edu.cn).

silicon produced on bulk and film substrates has the advantage that it could be used to realize light-emitting devices through the standard semiconductor fabrication process. Wu et al. first reported visible photoluminescence (PL) with a peak wavelength varying between 540 nm and 630 nm from black silicon, which was fabricated by 1-kHz fs-laser irradiation of bulk Si in an air atmosphere [5]. Later, two PL bands at 680 nm and 600 nm were observed from the black silicon that was fabricated by using high-repetition-rate fs-laser irradiation in air [6]. Emelyanov et al. reported visible luminescence from hydrogenated amorphous silicon modified by femtosecond laser radiation [7]. Although the emission wavelengths were different, the emission mechanisms for the above observed PL were attributed to the formation of Si nanocrystals embedded in a silica matrix. A consensus has been reached that highly localized defects at the Si/SiO<sub>2</sub> interface [8] and the quantum confinement (QC) of excitons both play important roles in the radiative emission from silicon nanocrystals embedded in a silica matrix[9, 10]. However, it is difficult to distinguish these two mechanisms experimentally [11]. Beyond luminescence in the visible range, strong infrared luminescence was also observed from black silicon formed by femtosecond laser radiation in an SF<sub>6</sub> atmosphere and consequent thermal annealing [12]. Until now, most research has reported on luminescence from silicon surface layers modified by femtosecond laser radiation; no reports have been published on luminescence from laser-induced structures inside silicon. In our previous study, we found that an 800-nm femtosecond laser could induce structure changes inside silicon, including embedded microchannels [13] and deep oxygen-doped regions [14]. Recently, we developed a new technology for fabricating high-aspect-ratio grooves by using wet etching to remove materials in oxygen-doped regions [15]. However, the physical properties of the femtosecond-modified region inside silicon (for example, the luminescence) are still unclear.

In this Letter, we report 680-nm PL from a femtosecond-laser-modified region inside silicon. Light-emitting structures were formed inside silicon by femtosecond laser irradiation in an air atmosphere. The formation of light-emitting structures arose from laser-induced oxygen doping (LIOD), and doping depths of a few hundred micrometers were able to be reached. The PL intensities and oxygen ratios decreased with increasing depth in the LIOD regions. PL intensities increased with increasing laser powers and with decreasing scanning velocities. After annealing at 1173 K and aging in air, the peak wavelength of PL almost remained constant. According to the Raman spectra results of

laser-treated specimens before and after annealing, the PL was attributed to the defect states at the interface between the silicon crystallites and the  $SiO_2$  matrix.

## II. EXPERIMENTS

<100> p-type silicon wafers with a thickness of 0.3 mm were used in our experiments. Laser treatment of silicon wafers was carried out with a Ti:sapphire laser system (Coherent Inc., Libra-USP-HE), which delivered pulses of 50-fs width with a repetition rate of 1 kHz and a wavelength centered at 800 nm. The laser beam was focused onto the specimen surface with a microscope objective (Nikon, 10×) that had a numerical aperture (NA) of 0.3. The focal spot size was estimated to be about 4.4 µm in diameter. The specimen was mounted on a three-dimensional translation stage and processed by scanning the focused laser radiation over the sample surface. After laser irradiation, the specimens were polished in a direction orthogonal to the surface from one edge of the surface to a random depth to observe the cross-section. The experimental setup and processing procedures have been previously described in greater detail in Ref. [14]. The PL spectra and Raman spectra measurements were carried out at room temperature by using a Micro-Raman spectrometer (Horiba Jobin Yvon HR800). A 5-mW laser with wavelength of 514 nm was used as an excitation source for PL and Raman spectra measurements. The exciting laser was focused via a microscope objective (Olympus, 100×, NA=0.9) onto the top and cross-sectional surface perpendicularly to measure the Raman and PL spectra of the LIOD regions at surface and different depths, respectively. The diameter of laser on specimen surface was about 1 µm. The specimens were annealed in Nitrogen ambient of 1 atmosphere by using an IR lamp heating system (ULVAC-RIKO RTP-6). The heating rate was programmed to be 30 °C/s. The morphology and chemical composition of the laser-treated silicon were characterized by a scanning electronic microscope (SEM, FEI Quanta 250 FEG Serials) equipped with an energy-dispersive X-ray spectrometer (EDS, TEAMTM Serials), respectively.

# III. RESULTS AND DISCUSSION

Figure 1 shows the morphologies of the surface and cross-section of laser-treated silicon. The specimen was made by using a femtosecond laser with a power of 50 mW and a scanning velocity of 5 µm/s, which corresponded to a laser fluence of 3.3 MJ/m<sup>2</sup> on the specimen surface and accumulated pulse numbers of 880 per beam spot area [5]. As shown in Fig. 1(a), microstructures were formed on the silicon surface after femtosecond laser irradiation. Structural change was also induced inside the silicon by the femtosecond laser as shown in Fig. 1(b), which included a high-aspect-ratio gray region below the surface and laser-induced microcavities at a depth of about 190 µm. EDS analysis indicated that oxygen was detected in the laser illuminated track. The formation of visible laser illuminated tracks was caused by the doping of the silicon with oxygen in the ambient air as a result of interaction between atmospheric oxygen and the laser irradiation. The oxygen concentration decreased with increasing depth and

decreased to zero at the depth where the microcavity appeared. The atomic concentrations of oxygen and silicon at the points shown in Fig. 1 were demonstrated in Table I. Accordingly, the atomic ratio of oxygen to silicon was calculated to be 1.24 at the surface (point 1). It decreased to 0.75 and 0.19 at depths of 40 µm (point 2) and 130 µm (point 3) in the LIOD region, respectively. According to five pieces of LIOD regions fabricated at the above condition, we obtained the average atomic ratios at surface and depths of 40 µm and 130 µm were about 1.55, 0.71 and 0.21, respectively. Moreover, we found that PL could be generated from the LIOD region inside the silicon. Figure 1(c) shows PL spectra from points 1, 2, and 3 under 514-nm laser excitation; the peak wavelengths of these spectra were at 680 nm. No PL was observed from pure monocrystal silicon. This indicates that the photoluminescence may originate from the oxidized silicon in the irradiated specimens. The absorption coefficients of silicon at 680 and 514 nm were 449.42 and 4060.2 cm<sup>-1</sup>. The penetration depth for PL and its exciting light was about 44.5 μm and 4.9 μm, respectively.

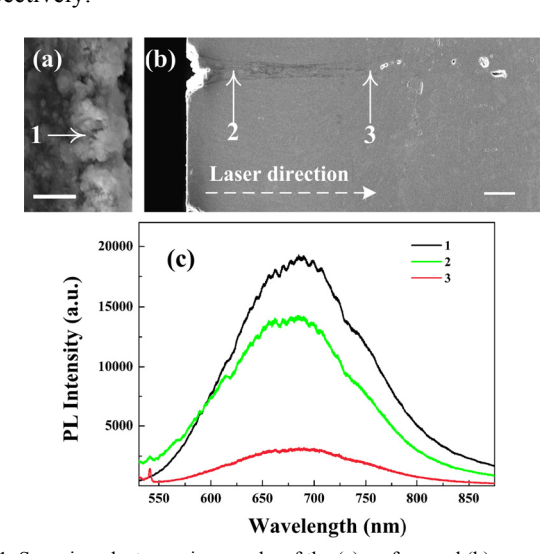


Fig. 1. Scanning electron micrographs of the (a) surface and (b) cross-section of laser-treated silicon. (c) PL spectra from the surface (point 1) and interior region (points 2 and 3) of laser-treated silicon. The scale bars in (a) and (b) are 2 and 20  $\mu$ m, respectively.

TABLE I

MEASURED OXYGEN AND SILICON CONCENTRATIONS AND THEIR
CALCULATED ATOMIC RATIOS AT DIFFERENT POSITIONS SHOWN IN FIG. 1

Position	Oxygen atomic concentration	Silicon atomic concentration	O/Si ratio
1	55.46%	44.54%	1.24
2	42.92%	57.08%	0.75
3	15.74%	84.26%	0.19

Then we studied the influence of the femtosecond laser power and the scanning velocity on the PL intensities. PL from the central point of the LIOD region 40  $\mu$ m beneath the silicon surface was measured for comparison. Figure 2(a) shows the PL spectra of silicon treated with different laser powers. The femtosecond laser powers were set to 10, 30, 40, and 50 mW, respectively. The scanning velocity was set to 5  $\mu$ m/s. The PL intensities increased with increasing femtosecond laser power while the PL peak remained at 680 nm. Figure 2(b) shows the PL spectra from specimens made at scanning velocities of 1, 5,

10, and 20  $\mu$ m/s and a laser power of 50 mW. It can be seen that the PL intensities decreased and that the PL peak always stayed at 680 nm as the scanning velocity increased. According to EDS analysis, the ratios of oxygen incorporated into the silicon increased with increasing laser power and decreasing scanning velocity [14, 15]. The dependences of PL intensities on the laser power and the scanning velocity shows similar tendency as that for oxygen ratio.

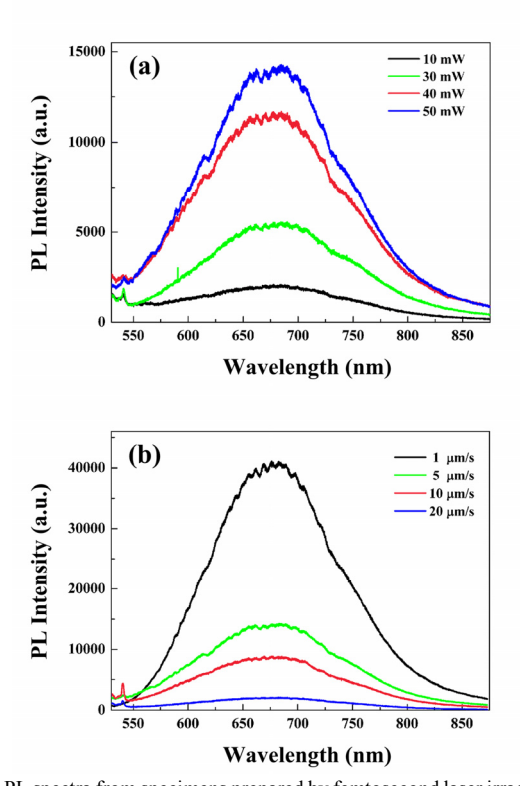


Fig. 2. PL spectra from specimens prepared by femtosecond laser irradiation at different laser powers and scan velocities. (a) Laser powers were set to 10, 30, 40, and 50 mW, respectively, and the scan velocity was set to 5  $\mu$ m/s. (b) The scan velocities was set to 1, 5, 10, and 20  $\mu$ m/s. The laser power was set to 50 mW.

Furthermore, we studied the effects of annealing in protective atmosphere and aging in air on PL to distinguish the PL mechanisms. The annealing or aging in air could change the nanocrystal size [16]. For "QC effect", peak wavelengths of PL increase with the decrease in the nanocrystal size while peak wavelengths usually keep constant for PL from defect states [11]. It was indicated that formation of amorphous Si clusters needs temperatures in excess of 837 K, and crystal silicon particle appears above 1087 K for silicon rich silica with O/Si<1 [17, 18]. Considering the limitation of maximum heating temperature of our IR lamp heating system, we annealed the specimens at 1173 K for 1 hour. This temperature was higher than the threshold temperature of 1087 K for silicon particle size change. The specimen was prepared at a laser power of 50 mW and a scan velocity of 5 µm/s. As shown in Fig. 3, the PL peak wavelength was still at 680 nm, but the intensities increased after annealing. Previously, C. Wu observed the appearance of a new PL band and its red shift after annealing at 1300 K for black silicon fabricated by using femtosecond laser irradiation [5]. Consequently, they contribute this PL band to the "QC effect". We believe that a different PL mechanism is at work in our experiments,

although the annealing temperatures used in our experiments and C. Wu's were different. Next we characterized the effect of aging on PL. After the annealed specimen was exposed to air for 3 months, the PL peak neither shifted as shown in Fig. 3. When silicon nanocrystals are exposed to air, their sizes gradually decrease due to the natural oxidization. Hence, the peak wavelength of PL shifts to the blue with gradual air exposure for "QC luminescence [16]." The results of aging effect neither obeyed the rules of the "QC effect".

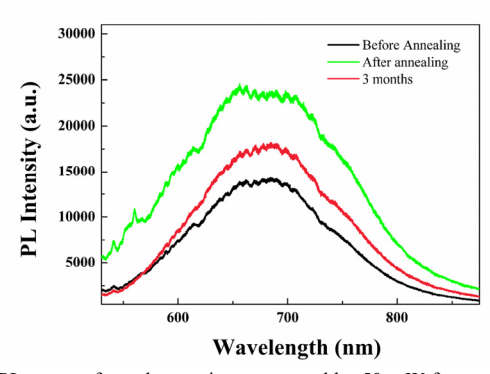


Fig. 3. PL spectra from the specimen prepared by 50-mW femtosecond laser irradiation before and after annealing at 1173 K for 1 hour and then after exposure to air for 3 months. The scan velocity was 5  $\mu$ m/s. The characterized region was the central point in the LIOD region 40  $\mu$ m beneath the silicon surface.

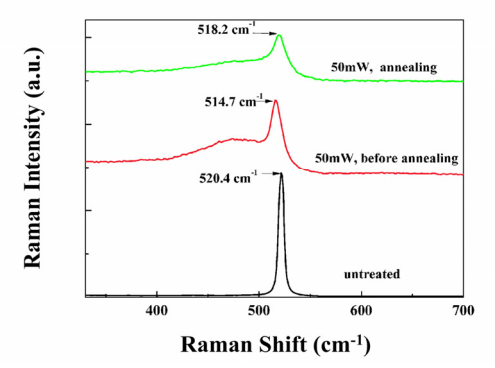


Fig. 4. Raman spectra of laser-treated silicon before (middle line) and after annealing (top line) at 1173 K for 1 hour and the Raman spectrum for untreated silicon. The specimen was prepared at a laser power of 50 mW and a scanning velocity of 5  $\mu$ m/s.

Furthermore, in order to clarify the PL mechanism in our experiments, Raman spectrum measurements were carried out to obtain structural information about the inside region of the laser-treated silicon. The Raman spectra corresponding to the PL analysis region in Fig. 3 and to untreated silicon are shown in Fig. 4. The Raman spectra for untreated silicon demonstrated a "crystal" line with a peak at 520.4 cm<sup>-1</sup>. In contrast, the Raman spectra of laser-treated silicon consisted of a broad band at low frequencies of about 480 cm<sup>-1</sup> that is related to amorphous silicon, and a narrow "crystalline" line that is attributed to silicon nanocrystals [18]. The peak positions of the "crystalline" lines for the specimens before and after annealing were shifted, respectively, by 5.7 cm<sup>-1</sup> (peak at 514.7 cm<sup>-1</sup>) and 2.2 cm<sup>-1</sup> (peak at 518.2 cm<sup>-1</sup>) with respect to that for untreated monocrystalline silicon.

For the PL due to quantum confinement, we were able to estimate the PL spectra peaks corresponding to the above Raman peak position shifts [19]. According to a confinement model, the Raman peak position decreased with the decrease in nanocrystal size. The Raman peak position shift caused by the confinement effect is described as follows [20]:

$$\Delta \omega = \omega(L) - \omega_0 = -A(a/L)^{\gamma}, \qquad (1)$$

where  $\omega(L)$  is the frequency of the Raman phonon in a Si nanocrystal with a size of L,  $\omega_0$  is the frequency of the optical phonon at the zone center, and a is the lattice constant of Si [20]. The parameters A and  $\gamma$  are used to describe the vibrational confinement due to the finite size in a nanocrystal, such as spheres, columns and so on [21]. For silicon spheres, the parameters A, a, and  $\gamma$  are 47.41 cm<sup>-1</sup>, 0.5431 nm, and 1.44, respectively [20], which were used in our estimates. Hence, the sizes of the silicon crystallites were calculated to be 2 nm and 5 nm, corresponding to the Raman shifts of 5.7 cm<sup>-1</sup> and 2.2 cm<sup>-1</sup> respectively. Such crystallites should give luminescence with peaks at about 620 nm and 800 nm according to the data present in Ref. [19]. This means that the PL peak positions should be very different before and after annealing if the origin of the PL was a "QC effect." However, the PL peak positions were almost unchanged. Thus, we have eliminated the possibility of QC PL, and the nanocrystals detected by Raman spectroscopy could not be responsible for the observed PL in our experiments. The origin of PL with a peak at 680 nm from the LIOD regions inside the silicon is most likely caused by the defect states between the silicon nanocrystals and SiO<sub>2</sub> matrix [7].

The formation of PL with different mechanisms in our experiments and Ref. [5] could be explained as follows. The LIOD regions included structures of nanocrystals, amorphous silicon and so on. C. Wu observed that PL from "QC effect" appeared after annealing at 1300 K. This PL may arise from nanocrystals formed due to crystallization of amorphous at high temperature. Although crystallization have occurred at 1173 K but the amount of formed nanocrystals was very low. In addition, the QC PL may be quenched by the defect PL [11]. Hence QC PL could only become prominent after annealing at high temperature. Moreover, the laser fluence used in our study was few hundred times larger than that used in Ref. [5], which could induce higher pressure and temperature in irradiated regions and introduce different defect states as compared with that for low laser fluence [5].

# IV. CONCLUSION

In summary, we observed 680-nm photoluminescence from the interior region of femtosecond laser-modified silicon. Oxygen in the ambient air was incorporated into silicon by femtosecond laser irradiation, and the light-emitting structures were formed in the LIOD region inside the silicon. The intensities of PL from the LIOD region decreased with increasing depth. The effects of laser powers and the scanning velocities on PL intensities were also investigated. The peak positions of the PL spectra were almost unchanged after annealing. According to the Raman spectroscopy analysis, PL from silicon originates in the defect states between the silicon nanocrystals and the  $SiO_2$  matrix.

### REFERENCES

- P. M. Fauchet, "Photoluminescence and electroluminescence from porous silicon," J. Lumin., vol. 70, pp. 294–309, 1996.
- [2] N. Mansour, A. Momeni, R. Karimzadeh, and M. Amini, "Blue-green luminescent silicon nanocrystals fabricated by nanosecond pulsed laser ablation in dimethyl sulfoxide," *Opt. Express*, vol. 2, no. 6, pp. Jun. 740–748.
- [3] D. Z. Tan, Z. J. Ma, B. B. Xu, Y. Dai, G. H. Ma, M. He, Z. M. Jin, and J. R. Qiu, "Surface passivated silicon nanocrystals with stable luminescence synthesized by femtosecond laser ablation in solution," *Phys. Chem. Chem. Phys.*, vol. 13, no. 45, pp. 20255–20261, Oct. 2011.
- [4] L. Pavesi, L. Dal Negro, C. Mazzoleni, G. Franzo, and F. Priolo, "Optical gain in silicon nanocrystals," *Nature*, vol. 408, no. 6811, pp. 440–444, Nov. 2000.
- [5] C. Wu, C. H. Crouch, L. Zhao, and E. Mazur, "Visible luminescence from silicon surfaces microstructured in air," *Appl. Phys. Lett.*, vol. 81, no. 11, pp. 1999–2001, Sep. 2002.
- [6] T. Chen, J. H. Si, X. Hou, S. Kanehir, K. Miura, and K. Hirao, "Luminescence of black silicon fabricated by high-repetition rate femtosecond laser pulses," *J. Appl. Phys.*, vol. 110, no. 7, pp. 073106, Oct. 2011.
- [7] A. V. Emelyanov, A. G. Kazanskii, M. V. Khenkin, P. A. Forsh, P. K. Kashkarov, M. Gecevicius, M. Beresna, and P. G. Kazansky, "Visible luminescence from hydrogenated amorphous silicon modified by femtosecond laser radiation" *Appl. Phys. Lett.*, vol. 101, no. 8, pp. 081902, Aug. 2012.
- [8] B. Averboukh, R. Huber, K. W. Cheah, Y. R. Shen, G. G. Qin, Z. C. Ma, and W. H. Zong, "Luminescence studies of a Si/SiO<sub>2</sub> superlattice," *J. Appl. Phys.* vol. 92, no. 7, pp. 3564–3568, Oct. 2002.
- [9] B. Dellley and E. F. Steigmeier, "Quantum confinement in Si Nanocrystals," *Phys. Rev. B*, vol. 47, no. 3, pp. 1397–1400, Jan. 1993.
- [10] S. Öğüt and James R. Chelikowsky, "Quantum confinement and optical gaps in Si nanocrystals," *Phys. Rev. Lett.*, vol. 79, no. 9, pp. 1770–1773, Sep. 1997.
- [11] S. Godefroo, M. Hayne, M. Jivanescu, A. Stesmans, M. Zacharias, O. I. Lebedev, G. Van Tendeloo, and V. V. Moshchalkov, "Classification and control of the origin of photoluminescence from Si nanocrystals", *Nature Nanotech.*, vol. 3, no. 3, pp. 174–178, Mar. 2008.
- [12] Q. Lu, J. Wang, C. Liang, L. Zhao, and Z. M. Jiang, "Strong infrared photoluminescence from black silicon made with femtosecond laser irradiation," *Opt. Lett.* 38, pp. 1274–1276, Apr. 2013.
- [13] T. Chen, J. H. Si, X. Hou, S. Kanehir, K. Miura, and K. Hirao, "Photoinduced microchannels inside silicon by femtosecond pulses," *Appl. Phys. Lett.*, vol. 93, no. 5, pp. 051112, Aug. 2008.
- [14] Y. C. Ma, H. T. Shi, J. H. Si, T. Chen, F. Yan, F. Chen, and X. Hou, "Photoinduced microchannels and element change inside silicon by femtosecond laser pulses," *Opt. Commun.*, vol. 285, no. 2, pp. 140–142, Jan. 2012.
- [15] A. Pan, J. H. Si, T. Chen, Y. C. Ma, F. Chen, and X. Hou, "Fabrication of high-aspect-ratio grooves in silicon using femtosecond laser irradiation and oxygen-dependent acid etching," *Opt. Express*, vol. 21, no. 14, pp. 16657–16662, Jul. 2013.
- [16] G. Ledoux, J. Gong, and F. Huisken, "Effect of passivation and aging on the photoluminescence of silicon nanocrystals," *Appl. Phys. Lett.* vol. 79, no. 24, pp. 4028–4030, Dec. 2001.
- [17] L. N. Nesbit, "Annealing characteristics of Si rich SiO2 films," Appl. Phys. Lett., vol. 46, no. 1, pp. 38-40, Jan. 1985.
- [18] M. Molinari, H. Rinnert, M. Vergnat, and P. Weisbecker, "Evolution with annealing treatments of the size of silicon nanocrystallites embedded in a SiN<sub>x</sub> matrix and correlation with optical properties," Mat. Sci. & Eng., B 101, 186-189, (2003).
- [19] G. Ledoux, J. Gong, F. Huisken, O. Guillois, and C. Reynaud, "Photoluminescence of size-separated silicon nanocrystals: Confirmation of quantum confinement," Appl. Phys. Lett. vol. 80, no. 25, pp. 4834–4836, Jun. 2002.
- [20] G. Viera, S. Huet, and L. Boufendi, "Crystal size and temperature measurements in nanostructured silicon using Raman spectroscopy," J. Appl. Phys. vol. 90, no. 8, pp. 4175–4183, Oct. 2001.
- [21] J. Zi, H. Buscher, C. Falter, W. Ludwing, K. Zhang, and X. Xie, "Raman shifts in Si nanocrystals," *Appl. Phys. Lett.* vol. 69, no. 2, pp. 200-202, Jul.1996.